23rd ABCM International Congress of Mechanical Engineering
December 6-11, 2015, Rio de Janeiro, RJ, Brazil

# ANALYSIS OF DISPLACEMENT FLOWS IN ANNULAR SPACE USING INTERFACE TRACKING METHOD

**Patrick P Dauelsberg**
**Frederico Carvalho Gomes**
**Marcio S Carvalho**
Departament of Mechanical Engineering
Pontifícia Universidade Católica do Rio de Janeiro – PUC-Rio
Rua Marquês de São Vicente, 225 – 22451-090 – Rio de Janeiro - Brazil
msc@puc-rio.br

***Abstract.*** *Cementing process is an important step in the construction of oil and gas wells. During cementing, it is necessary to displace the drilling mud by the cement slurry. Therefore, it is common to have three or more liquids flowing through the eccentric annular space. Non-uniform liquid displacement may lead to severe problems to the well structure and safety. A previous model developed a lubrication based model coupled with a level-set type method to simulate this process. However, when the interface deformation is large, such as in situations where buoyancy driven instabilities occur, the method led to large errors. Here, we propose a method at which the interface is tracked by material points placed along the initial configuration of the meniscus. The method greatly improved the accuracy of the predictions and is able to describe flow situations with very large interface deformation.*

***Keywords:*** *cementing process, interface tracking, lubrication model*

## 1. INTRODUCTION

The cementing process consists in filling the gap between the steel casing and the well-bore with cement and represents an essential stage while drilling a new well. Besides providing hydraulic seal, cementing promotes adhesion between the wall and the casing, provides structural support and isolates casing for subsequent drilling. Frequently, when cement flow rate is too low or pumping must be interrupted, buoyancy forces rule the flow, causing big distortions on the interface. This may lead to failures in the cementing process and severe problems which may risk productivity and security.

Gomes and Carvalho (2009) developed a lubrication based model coupled with a level-set type method (colour map) to simulate this process. The model is tested for cases where viscous forces lead the flow and big distortions on the interface do not occur.

Puckett *et al.* (1997) focused on the volume-of-fluid interface tracking method. In this model the loss of mass caused by diffusion in level set methods is solved. For a given velocity field the advancement of the interface is calculated satisfying a second-order unsplit advection algorithm. The interface in each cell is stipulated according to the volume of fluid in each cell using the least squares volume-of-fluid interface reconstruction algorithm. With this model, precise results were achieved, however it relies on refined grids to decrease discontinuities of the interface between cells.

Chen *et al.* (1997) developed a model based on pressure potential in which cells are divided into micro-cells in order to obtain a better definition of the location of the free surface. The model greatly improved it's predecessor Marker and Cell method, however the subdivision of the cells compromises computational cost and still presents discontinuities between micro cells which may be too big for complex flow.

The objective of this work is to develop a transport model based on lubrication theory to study the displacement of different liquids through an annular space with variable eccentricity, capable of simulating complex interfaces and phase inversions, without the need of a refined grid and associated prohibitive high computational cost.

## 2. Pressure and velocity field calculation

A dimensional analysis can be used to eliminate terms in the momentum and continuity equations for incompressible fluids, this procedure is known as lubrication approximation. Comparing the terms using typical scale lengths, the equations reduces to:

$$-\frac{\partial p}{\partial z}+\left[\frac{1}{r}\frac{\partial}{\partial r}\left(\mu r\frac{\partial u}{\partial r}\right)\right]-\rho g\sin\alpha=0 \tag{1}$$

$$-\frac{1}{r}\frac{\partial p}{\partial \theta} + \frac{\partial}{\partial r}\left[\frac{1}{r}\frac{\partial}{\partial r}(\mu r w)\right] - \rho g \cos\alpha \cos\theta = 0 \tag{2}$$

$$-\frac{\partial p}{\partial r} = 0 \tag{3}$$

$$\frac{\partial u}{\partial z} + \frac{1}{r}\frac{\partial w}{\partial \theta} = 0 \tag{4}$$

Using proper boundary conditions to determine the velocity profiles and integrating the mass conservation terms along the radius using Leibnitz's rule, we obtain the flow rate conservation equation:

$$\frac{\partial}{\partial z}\left[C_1\frac{\partial p}{\partial z} + C_2\right] + \frac{\partial}{\partial \theta}\left[C_3\frac{\partial p}{\partial \theta} + C_4\right] = 0 \tag{5}$$

where $C_1, C_2, C_3$ and $C_4$ depend on the properties of the fluids and the geometry of the well.

$$C_1 = \frac{1}{16\mu}\left[\frac{(R_e^2 - R_i^2)^2}{\ln\frac{R_e}{R_i}} - R_e^4 - R_i^4\right] \tag{6}$$

$$C_2 = C_1 \rho g \sin\alpha \tag{7}$$

$$C_3 = \frac{1}{2\mu}\frac{1}{R_e^2 - R_i^2}\left[\frac{(R_e^2 - R_i^2)^2}{4} - R_e^2 R_i^2 \ln^2\frac{R}{R_i}\right] \tag{8}$$

$$C_4 = \frac{\rho g z \cos\alpha \cos\theta}{3}\left[\frac{R_i^3 - R_e^3}{6} + \frac{R_e^2 R_i^2}{R_i + R_e}\ln\frac{R_e}{R_i}\right] \tag{9}$$

$R_i$ and $R_e$ are the internal and external radius respectively.

The velocities are calculated usinig an area weighted average:

$$U = \frac{1}{A}\int_{R_i}^{R_e} U dA \tag{10}$$

$$W = \frac{1}{A}\int_{R_i}^{R_e} U dA \tag{11}$$

$$U = \frac{2}{{R_e}^2 - R_i^2}\int_{R_i}^{R_e} urdr \tag{12}$$

$$W = \frac{1}{R_e - R_i}\int_{R_i}^{R_e} wdr \tag{13}$$

$$U = \frac{2}{{R_e}^2 - R_i^2}\left(C_1\frac{\partial P}{\partial z} + C2\right) \tag{14}$$

$$W = \frac{2}{{R_e}^2 - R_i^2}\left(C_1\frac{\partial P}{\partial z} + C2\right) \tag{15}$$

## 3. Transport model

The idea of this transport model is to track the interface using massless markers, which are free to move inside the cells and, at each time step, calculate the relative area occupied by each fluid in each cell. This model addresses multiphase flow as a single phase with multiple properties. There are no specific boundary conditions on the interfaces and the pressure field is calculated using fluid and geometrical informations at each cell.

As buoyancy driven flows are very sensitive to density changes, precision is necessary when related to it. The physical properties are easily calculated in cells containing only one fluid, however, cells crossed by the interface present multiple phases, making this evaluation more challenging and requiring the calculation of equivalent properties.

Using the interface geometry, the relative area occupied by each fluid in the cells is calculated. With this information it is possible to evaluate the equivalent properties using an area weighted average. The markers positions are described by 2 time-variable vectors, thus allowing the formation of more complex interfaces, which cannot be described by a single variable. The model can be divided into 4 parts:

### 3.1 Velocity field interpolation

Markers are updated according to their specific velocities. As the calculated velocity field is discrete and the cells distance is much larger than the interval between two adjacent markers, it is necessary the interpolation of the velocities. For this purpose, Lagrange interpolators were adapted for the 2 dimensional space to create a function of the type

$$\overrightarrow{V}(M,N) = aM + bN + cMN + d \tag{16}$$

Where $\overrightarrow{V}(M,N)$ is a generic velocity vector. N and M are the normalized longitudinal and latitudinal coordinates inside the cell.

The bi-dimensional Lagrange interpolator functions are:

$$\phi_1 = (N-1)(M-1) \tag{17}$$
$$\phi_2 = (1-N)(M) \tag{18}$$
$$\phi_3 = MN \tag{19}$$
$$\phi_4 = N(1-M) \tag{20}$$
$$\tag{21}$$

The interpolators are multiplied by the nominal velocities located in the 4 corners of the cell to determine the interpolated velocity at each position.

$$\overrightarrow{V}(M,N) = \phi_1\overrightarrow{V}_1 + \phi_2\overrightarrow{V}_2 + \phi_3\overrightarrow{V}_3 + \phi_4\overrightarrow{V}_4 \tag{22}$$

Where $\overrightarrow{V}_1$ ,$\overrightarrow{V}_2$ ,$\overrightarrow{V}_3$ and $\overrightarrow{V}_4$ are the velocities in the corners of the cell.

A different function is generated at each cell, but as the velocity profile in the boundaries is always a straight line connecting the nominal velocities in the corners, it is possible to connect the profiles in the edges of the cells, creating a continuous velocity field.

### 3.2 Marker's position update

As buoyancy driven flows may present very different characteristic velocities over time, it is interesting to create a variable time step. The time interval is calculated as a function of the maximum velocity magnitude in order to avoid big markers movement during a single time step and also avoid many calculations for a stagnated flow. Finally, the evolution of the fluid's free surface is accomplished by moving the markers to new locations according to

$$\overrightarrow{X}_{t+\delta t} = \overrightarrow{X}_t + \delta t_t \overrightarrow{V}_t \tag{23}$$

### 3.3 Interface geometry analysis

In this step of the model, the interface vector is fully analyzed and important markers and parameters are created according to the geometry. The interfaces bounded by the walls of the cells are approximated by polygons and markers are added to adequate the geometries. Additional markers are placed where precision is more necessary and deleted when not. This is the most extensive part of the program, as numerous conditions are necessary to cover each possible geometry of the interface.

### 3.4 Area calculation

Using the parameters obtained in the previous step, the area of each polygon is calculated according to

$$\frac{1}{2}|\sum_{z=1}^{n-1} x_z y_{z+1} - x_{z+1} y_z| \tag{24}$$

Where $x$ and $y$ are the vectors containing the x and y coordinates of the markers.

Some criteria were created to track errors caused by highly complex geometries, out of the application range of this model. The areas may be imprecisely calculated when the interface crosses the same cell more than four times. A wrongly calculated area at time $t$ is substituted by its calculation at time $t - \delta t$.

The final part of the program is the creation of the phase matrix, where the concentration of each fluid is written in their respective cells. For the pressure field calculation in the next step, the program uses the phase matrix in order to obtain the right calculation of each equivalent physical property, thus obtaining better results.

## 4. RESULTS

The referential used in the graphics and data is explained in the figure below:

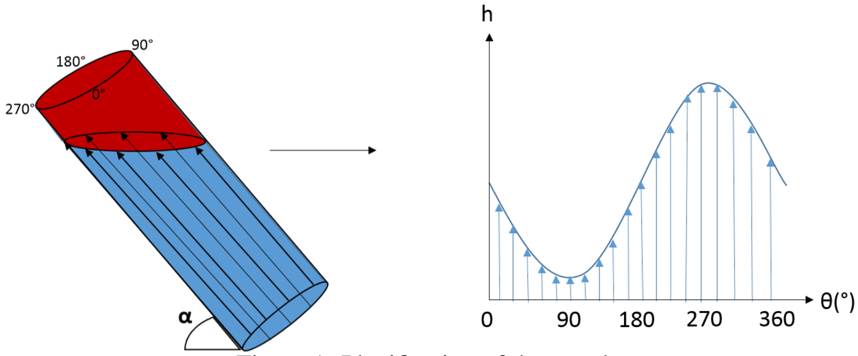


Figure 1: Planification of the annular

### 4.1 Case 1

A technique known as directional drilling consists in drilling non-vertical wells. Its benefits include increasing exposed section length through the reservoir and allowing more wellheads to be grouped together on one surface location. In the other hand, inclined wells may lead to a gravitational stratification of fluids, which can lead to even worse results if the upper fluid has greater density than lower fluid. To simulate the directional drilling, case 1 is an example of inclined eccentric annular with the geometry defined as shown in table 1. Two Newtonian fluids with properties specified in table 4 are pumped. The lower fluid has lower density than the upper fluid, which originally occupied the annular space. This case was simulated using the model presented here and compared with the older transport model (colour map).

| | |
|---|---|
| $N\theta$ | 30 |
| Nz | 30 |
| L [m] | 100.0 |
| $R_0$ [m] | 0.1143 |
| $R_i$ [m] | 0.1020 |
| $e_1$ [m] | 0.001 |
| $e_2$ [m] | 0.001 |
| $\alpha[deg]$ | 72 |

Table 1: Geometry Data – Case 1

| - | $\mu[Pa.s]$ | $\rho[kg/m^3]$ | $Q[m^3/s]$ |
|---|---|---|---|
| Upper fluid | 0.015 | 1500.00 | 0.0850 |
| Lower fluid | 0.015 | 1000.00 | 0.0850 |

Table 2: Fluids Data – Case 1

The high pumping rate in this case superimposes the buoyancy forces caused by different densities, therefore the older model is capable of simulating it with satisfactory precision. However this comparison shows that the new model predicted with more details the finger induced by instable conditions. In fact, there are in the older model non conservative imprecisions which can be dangerous when the simulation is necessary to take important decisions.

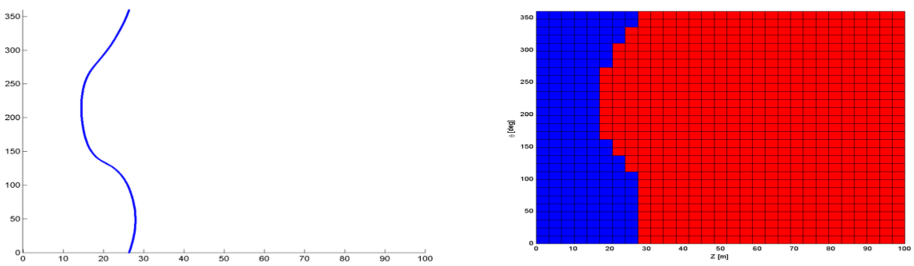

(a) New Model (b) Old Model

Figure 2: t1

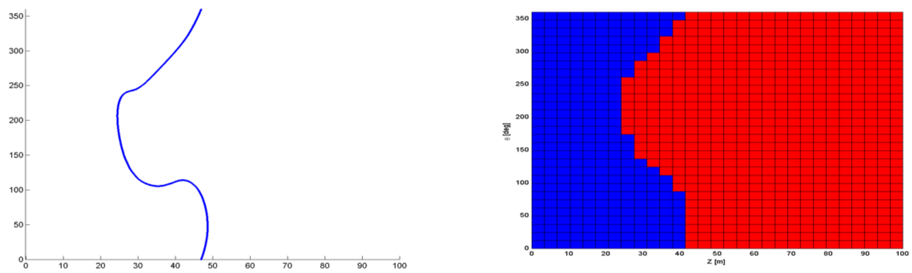

(a) New Model (b) Old Model

Figure 3: t2

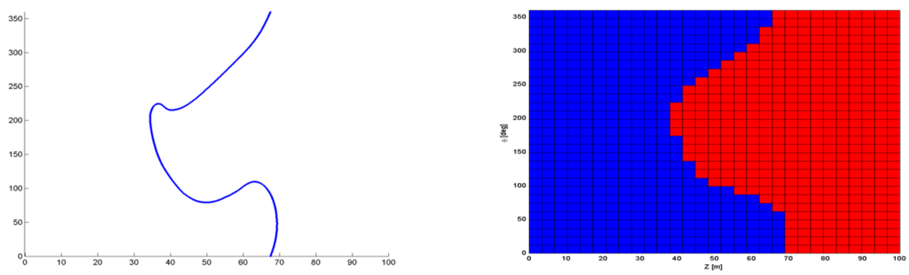

(a) New Model (b) Old Model

Figure 4: t3

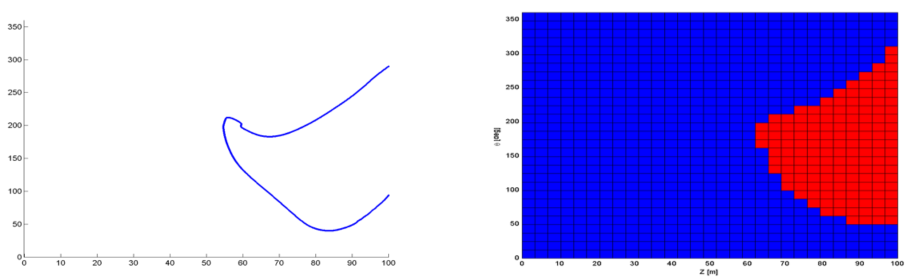

(a) New Model (b) Old Model

Figure 5: t4

### 4.2 Case 2

Case 2 simulates two fluids initially stationary in a concentric, inclined well with no pumping process. The interface is initially set in the middle of the total well height. The upper fluid has higher density, therefore it is expected to flow through the lower side of the annular towards the bottom. Furthermore, because of the concentricity, there must be symmetry in respect to the vertical plane (90° - 270°).

The new model has slightly higher computational cost, thus the meshes were adapted in order to equalize simulation time and enable a fair comparison. An unrefined mesh was used to compare the models at an extreme case.

The properties of the fluids and geometry of the well are presented on the tables below:

| | |
|---|---|
| $N\theta$(old) | 31 |
| Nz(old) | 31 |
| $N\theta$(new) | 25 |
| Nz(new) | 25 |
| L [m] | 100.0 |
| $R_0$ [m] | 0.1143 |
| $R_i$ [m] | 0.1043 |
| $e_1$ [m] | 0 |
| $e_2$ [m] | 0 |
| $\alpha[deg]$ | 72 |

Table 3: Geometry Data – Case 2

| - | $\mu[Pa.s]$ | $\rho[kg/m^3]$ | $Q[m^3/s]$ |
|---|---|---|---|
| Upper fluid | 0.015 | 2000.00 | 0 |
| Lower fluid | 0.015 | 1800.00 | 0 |

Table 4: Fluids Data – Case 1

The figures below show a close up view of the interfaces at a certain time during the phases inversion. Note that the interface shown in Fig. 6a is represented by only 5 cells in the longitudinal direction. Figure 6b shows that the older model is not suitable for such conditions.

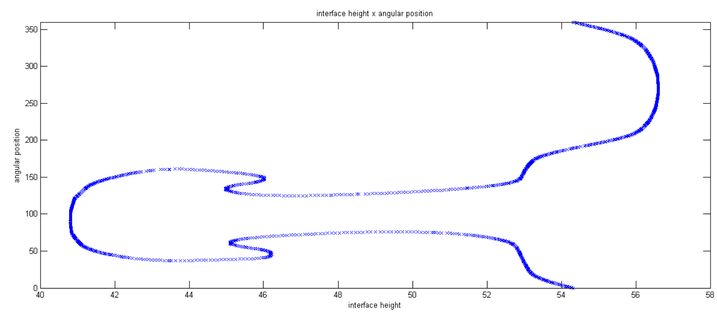


(a) New Model

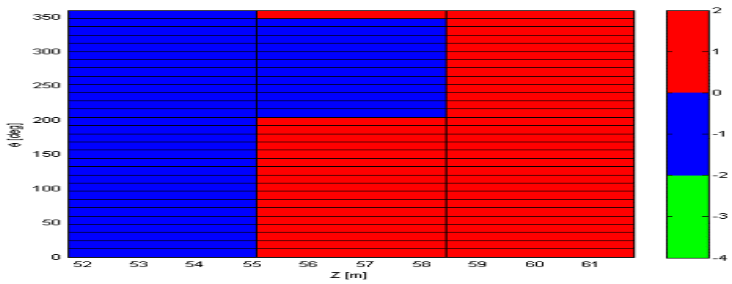


(b) Old Model

Figure 6: Phase inversion

## 5. CONCLUSIONS

A numerical method for approximating solutions of the incompressible bi-dimensional Navier-Stokes equations was presented for two fluids with different properties. It was demonstrated that the interface tracking algorithm is able to generate precise results by converting discrete position and velocity fields into continuous fields, not constraining the interface to the edges of the cells. Furthermore, in this model, equivalent physical properties of the fluids are calculated in the cells crossed by the interface, enabling a proper discrete representation of the continuous interface, thus producing more precise results when calculating the pressure field. The results showed precise interfaces, even when unrefined grids are used.

## 6. REFERENCES

Chen, S., Johnson, D.B., Raad, P.E. and Fadda, D., 1997. "The surface marker and micro cell method". *International Journal for Numerical Methods in Fluids*, Vol. 25, No. 7, pp. 749–778.

Gomes, F. and Carvalho, M., 2009. "Lubrication model for the flow of several liquids through an annular space with varying eccentricity". In *Proceedings of COBEM*.

Puckett, E.G., Almgren, A.S., Bell, J.B., Marcus, D.L. and Rider, W.J., 1997. "A high-order projection method for tracking fluid interfaces in variable density incompressible flows". *Journal of Computational Physics*, Vol. 130, No. 2, pp. 269–282.

## 7. RESPONSIBILITY NOTICE

The author(s) is (are) the only responsible for the printed material included in this paper.